

Dynamics of position disordered Ising spins with a soft-core potential

Canzhu Tan,^{1,2} Xiaodong Lin,^{1,2} Yabing Zhou,^{1,2} Y. H. Jiang,^{3,2} Matthias Weidemüller,^{1,2,4} and Bing Zhu^{4,2,*}

¹*Hefei National Laboratory for Physical Sciences at the Microscale and Shanghai Branch,
University of Science and Technology of China, Shanghai 201315, China*

²*CAS Center for Excellence and Synergetic Innovation Center in Quantum Information and Quantum Physics,
University of Science and Technology of China, Shanghai 201315, China*

³*Shanghai Advanced Research Institute, Chinese Academy of Sciences, Shanghai 201210, China*

⁴*Physikalisches Institut, Universität Heidelberg, Im Neuenheimer Feld 226, 69120 Heidelberg, Germany*

(Dated: November 2, 2021)

We theoretically study magnetization relaxation of Ising spins distributed randomly in a d -dimension homogeneous and Gaussian profile under a soft-core two-body interaction potential $\propto 1/[1 + (r/R_c)^\alpha]$ ($\alpha \geq d$), where r is the inter-spin distance and R_c is the soft-core radius. The dynamics starts with all spins polarized in the transverse direction. In the homogeneous case, an analytic expression is derived at the thermodynamic limit, which starts as $\propto \exp(-kt^2)$ with a constant k and follows a stretched-exponential law at long time with an exponent $\beta = d/\alpha$. In between an oscillating behaviour is observed with a damping amplitude. For Gaussian samples, the degree of disorder in the system can be controlled by the ratio l_ρ/R_c with l_ρ the mean inter-spin distance and the magnetization dynamics is investigated numerically. In the limit of $l_\rho/R_c \ll 1$, a coherent many-body dynamics is recovered for the total magnetization despite of the position disorder of spins. In the opposite limit of $l_\rho/R_c \gg 1$, a similar dynamics as that in the homogeneous case emerges at later time after a initial fast decay of the magnetization. We obtain a stretched exponent of $\beta \approx 0.18$ for the asymptotic evolution with $d = 3, \alpha = 6$, which is different from that in the homogeneous case ($\beta = 0.5$).

PACS numbers:

I. INTRODUCTION

Disorder plays an essential role in determining both equilibrium and non-equilibrium properties of a many-body system, e.g. glassy phase and dynamics in magnetics [1], localization phenomenon of transports [2], and novel materials by disorder engineering [3–5]. While knowing very details of a disordered system is difficult and not necessary, understanding its universal behaviour starting from a microscopic Hamiltonian is important to pin down the underlying physics. For example, many relaxations in glass materials (normal or spin-type) follow a simple stretched-exponential law ($\propto \exp[-(\gamma t)^\beta]$, $\beta < 1$) [1, 6]. Klafter and Shlesinger found that a scale-invariant distribution of relaxation times was the common underlying structure for three different physical models showing a stretched-exponential decay [7], which was generalized to closed quantum systems by Schultzen and coworkers recently [8].

For a disordered spin-1/2 system, recent studies confirmed a stretched-exponential decay of magnetization in both Ising [8] and Heisenberg [9, 10] models, where the pairwise spin-spin interaction exhibits a power-law dependence on the inter-spin distance r , $J(r) \propto 1/r^\alpha$ with $\alpha \geq d$ in the d -dimension. The scale invariance is guaranteed since pairwise contribution to the relaxation dynamics is determined by $J(r)t$, which is invariant under the following rescaling of space and time: $r \rightarrow \lambda r$ and

$$t \rightarrow \lambda^\alpha t.$$

How would the stretched-exponential law change if the scale invariance is broken? Here we consider a specific type of pairwise interactions in an Ising Hamiltonian, namely a soft-core potential $J(r) \propto 1/[1 + (r/R_c)^\alpha]$ with $\alpha \geq d$ and R_c the soft-core radius, reducing to the power-law behaviour at large r . We have studied two different situations: (i) For homogeneously distributed spins, an analytical formula is derived for the magnetization relaxation at the thermodynamic limit, which features three different regions in the time axis: The dynamics starts as $\propto \exp(-kt^2)$, followed by an oscillating decay, and eventually obeys an stretched-exponential law. (ii) For a spatially inhomogeneous sample, e.g. Gaussian distributed, a coherent many-body dynamics is observed in small-spatial-size system while disorder-induced relaxation is recovered for large spatial sizes. Our investigation concerning the soft-core potential is inspired by Rydberg dressing in cold-atom experiments (for recent reviews see [11, 12]) and both studied situations can be readily tested there; A uniform gas can be prepared via box potentials [13, 14] and a Gaussian distribution of atoms is obtained with a harmonic trap [15].

The article is organized as follows: We derive and discuss the analytical result for homogeneous samples in Sec. II B. The inhomogeneous situation is numerically investigated in Sec. II C and Sec. III concludes the paper.

*Electronic address: bzhu@physi.uni-heidelberg.de

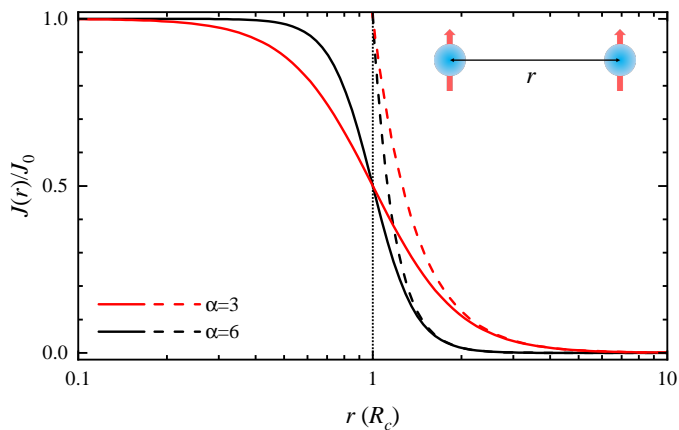


FIG. 1: Soft-core interaction potential between two spin-up particles. The soft-core potential in Eq. (2) is plotted as a function of inter-spin distance r with $\alpha = 3$ and 6 (solid curves). As a comparison, the power-law interactions $J_0/(r/R_c)^\alpha$ are also shown.

II. DISORDERED ISING MODEL WITH A SOFT-CORE POTENTIAL

A. The Ising Hamiltonian and its dynamics

A general Ising Hamiltonian for N spin-1/2 particles reads

$$\hat{H}_{\text{Ising}} = \frac{1}{2} \sum_{i,j} J_{ij} \hat{\sigma}_i^z \hat{\sigma}_j^z, \quad (1)$$

where $\hat{\sigma}_{i(j)}^z$ is the Pauli z operator and J_{ij} is the coupling strength between spins i and j . J_{ij} takes a form of the soft-core potential

$$J_{ij} \equiv J(r_{ij}) = \frac{J_0}{1 + (r_{ij}/R_c)^\alpha}, \quad (2)$$

where the long-range part ($r_{ij} \gg R_c$) has a power-law form ($\propto 1/r_{ij}^\alpha$) and the short-range ($r_{ij} \ll R_c$) interaction is almost a constant J_0 , as seen in Fig. 1. Such a potential is not invariant under the spatial scaling $r \rightarrow \lambda r$ in general, while it is approximately invariant at large $r \gg R_c$. We will see later that this leads to a stretched-exponential relaxation for long-time dynamics both in the analytic solution of a homogeneous sample and the numerical results of a Gaussian one.

We focus on dynamics of the mean magnetization $\langle \hat{S}_x(t) \rangle = \langle \sum_{i=0}^N \hat{\sigma}_x^i(t) \rangle / N$ with a initial state that all spins are polarized in the $+x$ direction $|\phi_0\rangle = |\rightarrow\rangle^{\otimes N}$ with $\hat{\sigma}_x |\rightarrow\rangle = +1 |\rightarrow\rangle$, i.e. $\langle \hat{S}_x(0) \rangle = 1$. Emch [16] and Radin [17] have obtained an analytical expression

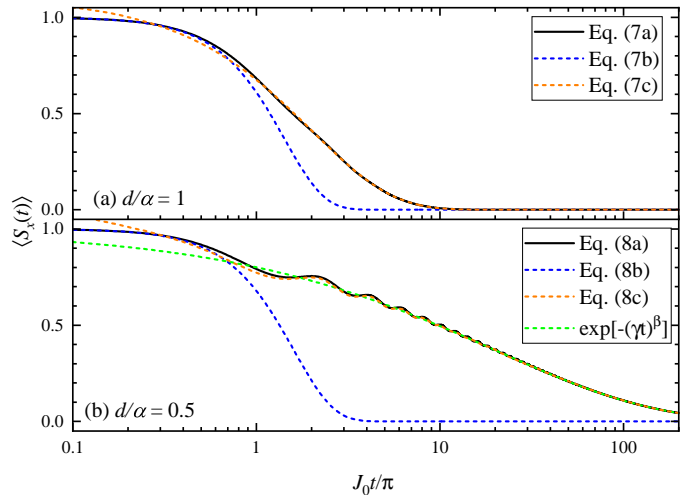


FIG. 2: Plots of analytic results for magnetization relaxation in uniformly distributed Ising spins under a pairwise soft-core interaction. (a) The case of $\beta_0 = d/\alpha = 1$. The black solid, blue dashed, and orange dashed curves represent the complete [Eq. (7a)], short-time asymptotic [Eq. (7b)], and long-time asymptotic [Eq. (7c)] expressions, respectively. (b) Similar as in (a) for the case of $\beta_0 = d/\alpha = 0.5$. We also show the stretched-exponential function as a green curve for comparison.

for $\langle \hat{S}_x(t) \rangle$ with the initial state $|\phi_0\rangle$, which reads as

$$\langle \hat{S}_x(t) \rangle = \sum_{i=1}^N 1/N \prod_{j \neq i} \cos(J_{ij}t). \quad (3)$$

All following analytical and numerical results are based on the above equation.

B. Homogeneous samples: the thermodynamic limit

We consider a system of N spins uniformly distributed in a spherical volume V in the d dimension. Following the same derivation procedure in Ref. [8], by replacing the ensemble average with an average over all possible configurations of placing $N - 1$ spins around a reference one at $\mathbf{r}_1 = \mathbf{0}$, Eq. (3) can be transformed to

$$\begin{aligned} \langle \hat{S}_x(t) \rangle &= \int_V d\mathbf{r}_2 \cdots d\mathbf{r}_N P(\mathbf{r}_2, \cdots, \mathbf{r}_N) \prod_{j=2}^N \cos(J_{1j}t) \\ &= \left\{ \frac{1}{V} \int_V d\mathbf{r} \cos[J(r)t] \right\}^{N-1} \\ &= \left\{ \frac{d}{r_0^d} \int_0^{r_0} r^{d-1} dr \cos\left[\frac{J_0 t}{1 + (r/R_c)^\alpha}\right] \right\}^{N-1} \end{aligned} \quad (4)$$

Here $P(\mathbf{r}_2, \cdots, \mathbf{r}_N) = 1/V^{N-1}$ is the probability of placing the $N - 1$ spins at positions $\mathbf{r}_2, \cdots, \mathbf{r}_N$, respectively, and $J(r)$ takes the form in Eq. (2).

For the power-law interaction ($\propto 1/r^\alpha$) a short-distance cutoff has to be introduced to avoid the divergence of interaction strength for further simplifying Eq. (4) [8], which is not necessary for the soft-core potential considered here. By introducing a new variable $y = J_0 t / [1 + (r/Rc)^\alpha]$ and integrating by parts, Eq. (4) can be written as

$$\langle \hat{S}_x(t) \rangle = [1 - \frac{\pi^{d/2} \rho R_c^d}{\Gamma(d/2 + 1) N} \int_{y_0}^{J_0 t} (J_0 t / y - 1)^{\beta_0} \sin y dy]^{N-1} \quad (5)$$

where $N = \rho V = \rho \pi^{d/2} r_0^d / \Gamma(d/2 + 1)$, $\beta_0 = d/\alpha$, and $y_0 = J_0 t / [1 + (r_0/Rc)^\alpha]$. Here ρ is the particle density and $\Gamma(x)$ is the Gamma function. In the thermodynamic limit ($N, r_0 \rightarrow \infty$ and ρ is a constant), the integral $I(J_0 t; \beta_0) = \int_{y_0}^{J_0 t} (J_0 t / y - 1)^{\beta_0} \sin y dy$ is finite only if $\beta_0 \leq 1$ and the above equation gives

$$\langle \hat{S}_x(t) \rangle = \exp[-FI(J_0 t; \beta_0)] \quad , \quad (6)$$

where $F = \pi^{d/2} \rho R_c^d / \Gamma(d/2 + 1)$.

Let us first consider $\beta_0 = 1$,

$$I(J_0 t; 1) = J_0 t \text{Si}(J_0 t) + \cos(J_0 t) - 1 \quad , \quad (7a)$$

where $\text{Si}(x) = \int_0^x \sin(t)/t dt$ is the sine integral function. At short times ($J_0 t \ll 1$),

$$I(J_0 t; 1) \sim 1/2(J_0 t)^2 \quad , \quad (7b)$$

while

$$I(J_0 t; 1) \sim \pi/2 J_0 t - 1 \quad (7c)$$

for long times ($J_0 t \gg 1$). In Fig. 2(a), all three formulae are plotted as a function of evolution time and Eqs. (7b) and (7c) describe excellently the asymptotic dynamics at short and long times, respectively. Specifically, a stretched-exponential decay, $\exp[-(\gamma t)^\beta]$ with $\beta = \beta_0 = 1, \gamma = J_0 F \pi/2$, is seen for the long-time dynamics.

Next we look at $\beta_0 < 1$, the integral $I(J_0 t; \beta_0)$ is

$$I(J_0 t; \beta_0) = J_0 t B(1 - \beta_0, 1 + \beta_0) \Im[{}_1F_1(1 - \beta_0, 2, iJ_0 t)] \quad , \quad (8a)$$

where $B(x, y)$ is the Euler beta function, ${}_1F_1(a, b, z)$ is the Kummer confluent hypergeometric function, and $\Im[z]$ gives the imaginary part of z . More details can be found in Appendix III. The asymptotic behaviors of Eq. (8a) are

$$I(J_0 t; \beta_0) \sim 1/2(J_0 t)^2(1 - \beta_0)B(1 - \beta_0, 1 + \beta_0) \quad (8b)$$

for short times ($J_0 t \ll 1$), and

$$I(J_0 t; \beta_0) \sim (J_0 t)^{\beta_0} [\cos(\beta_0 \pi/2) \Gamma(1 - \beta_0) - (J_0 t)^{-2\beta_0} \cos(J_0 t - \beta_0 \pi/2) \Gamma(1 + \beta_0)] \quad (8c)$$

for long times ($J_0 t \gg 1$).

The asymptotic form of Eq. (8b) for $\beta_0 \rightarrow 1$ actually coincides with Eq. (7b). Thus, for $\beta_0 \leq 1$ the initial dynamics of $\langle \hat{S}_x(t) \rangle$ follows $\exp[-kt^2]$ with $k = J_0^2 F(1 - \beta_0)B(1 - \beta_0, 1 + \beta_0)/2$. In the long-time limit, the second term inside the square bracket in Eq. (8c) can be neglected and the first term has an asymptotic value of $\pi/2$ for $\beta_0 \rightarrow 1$. So the long-time behaviour of $\langle \hat{S}_x(t) \rangle$ is a stretched exponential $\exp[-(\gamma t)^\beta]$ with $\beta = \beta_0$ and $\gamma = J_0 [F \cos(\beta_0 \pi/2) \Gamma(1 - \beta_0)]^{1/\beta_0}$. As a specific example, we show plots of Eq. (6) with $I(J_0 t; \beta_0)$ from Eqs. (8a), (8b), and (8c) in Fig. 2(b) for $\beta_0 = 0.5$. Other than the two limits discussed before, a damped oscillating decay is observed in between, which to a large extent can be captured by the neglected second term inside the square bracket in Eq. (8c). This oscillating decay signatures the breakdown of scale invariance with the soft-core potential.

C. Gaussian samples: a numerical study

To extend the above analytic result for the homogeneous case, we numerically investigate the magnetization relaxation for an inhomogeneously distributed spin sample (Gaussian distributed) in this section, where the degree of disorder can be tuned. We focus on dynamics of the magnetization $\langle \hat{S}_x(t) \rangle$ under the setting specified in Sec. II A, however, with spin positions $\mathbf{r} = (x, y, z)$ randomly distributed in a three-dimension Gaussian distribution ($d = 3$)

$$G(\mathbf{r}) = \frac{1}{(2\pi)^{3/2} w_x w_y w_z} \exp\left(-\frac{x^2}{2w_x^2} - \frac{y^2}{2w_y^2} - \frac{z^2}{2w_z^2}\right) \quad , \quad (9)$$

where w_η is the Gaussian waist in η direction ($\eta \in \{x, y, z\}$). This distribution of spins could be realized with ultracold atoms trapped in harmonic traps [15]. The mean particle density is $\rho = N/(8\pi^{3/2} w_x w_y w_z)$ with the total particle number N and for simplicity we assume $w_x = w_y = w_z \equiv w$, giving rise to a mean inter-spin dis-

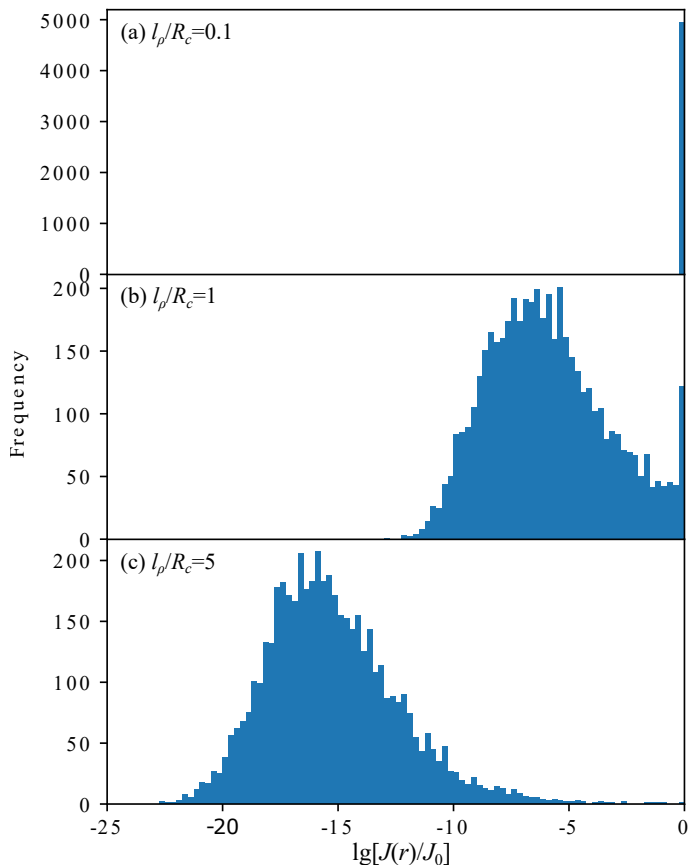


FIG. 3: Distribution of the pair interaction strength $J(r)$ for 100 spins randomly distributed in a three-dimensional Gaussian profile. (a), (b), (c) show the distribution of $\lg[J(r)/J_0]$ for a mean interparticle distance of $l_\rho/R_c = 0.1, 1, 5$, respectively.

tance of $l_\rho \equiv \rho^{-1/3} = 2\sqrt{\pi}w/N^{1/3}$ and its corresponding interaction strength $J_\rho = J(l_\rho) = J_0/[1+(\pi^{d/2}/F\Gamma(d/2+1))^{1/\beta_0}]$ in Eq. (2) with F, β_0 defined in Sec. II B. For following numeric calculation, we fix the total spin number $N = 100$ and $\alpha = 6$ ($\beta_0 = 0.5$).

For the soft-core potential in Eq. (2), R_c separates the interaction-strength randomness into two different regimes according to the ratio l_ρ/R_c for the above Gaussian sample. We show in Fig. 3 the distribution of pair interaction strengths with 100 spins randomly distributed according to Eq. (9) for three different values of l_ρ/R_c : 0.1, 1, and 5. When l_ρ is much smaller than R_c [$l_\rho/R_c = 0.1$ in Fig. 3(a)], $J(r)$ is almost the constant J_0 for all pairs, hence randomness is minimized. Otherwise when $l_\rho/R_c \gtrsim 1$, the distribution of $J(r)$ spans over several orders of magnitude, as seen in Figs. 3(b, c). Thus effects arising from disorder are expected to be important in this regime.

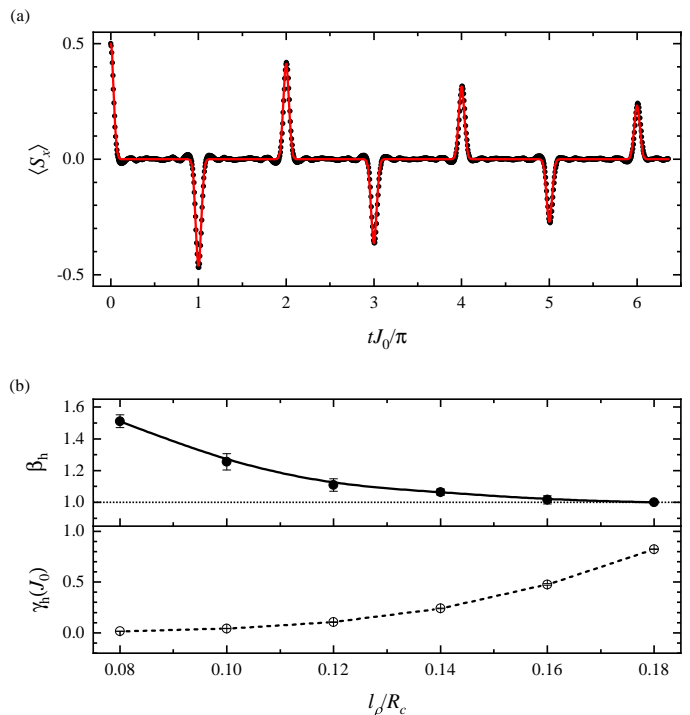


FIG. 4: Magnetization dynamics in a high-density Gaussian sample. (a) The time evolution of mean magnetization $\langle \hat{S}_x \rangle$ (solid points) for $l_\rho/R_c = 0.1$. After an initial fast decay, quantum revivals are observed with a damped amplitude. The red curve is a fit to the function of $\cos^{N-1}(J_0 t) \exp[-(\gamma_h t)^{\beta_h}]$ (see text for details), with which the stretched exponent β_h and decay rate γ_h are extracted. (c) The fitted β_h and γ_h as a function of l_ρ/R_c . The lines are guides to eyes. See text for more discussions.

1. High-density regime

In Fig. 4 we present the numerical results from Eq. (3) for $l_\rho/R_c \in (0.1, 0.2)$ ($\rho \sim 10^{14} - 10^{15} \text{ cm}^{-3}$ for $R_c = 1 \mu\text{m}$), coined *high-density regime*. In this regime, the system behaves like a all-to-all interacting one with a single interaction strength J_0 [18], recovering a coherent many-body dynamics, as seen in Fig. 4(a) for the magnetization dynamics with $l_\rho/R_c = 0.1$. A fast initial decay of magnetization due to the buildup of correlations [19, 20] and periodic quantum revivals with decaying amplitudes are observed.

In Eq. (3), if all the interaction strengths take a common value of J_0 , the resulting dynamics of $\langle \hat{S}_x(t) \rangle$ has an analytic form, $\langle \hat{S}_x(t) \rangle = \cos^{N-1}(J_0 t)$, giving rise to a coherent many-body quantum-revival dynamics [18]. To account for the observed decaying revival dynamics in Fig. 4(a), we phenomenologically fit the numerical data to a form of $\cos^{N-1}(J_0 t) \exp[-(\gamma_h t)^{\beta_h}]$, which is a stretched-exponential decay and shown as the red curve in the figure. Note that we have tried fits with a pure exponential decay, which can not fully capture the observed dynamics. From the fit, we obtain the stretched expo-

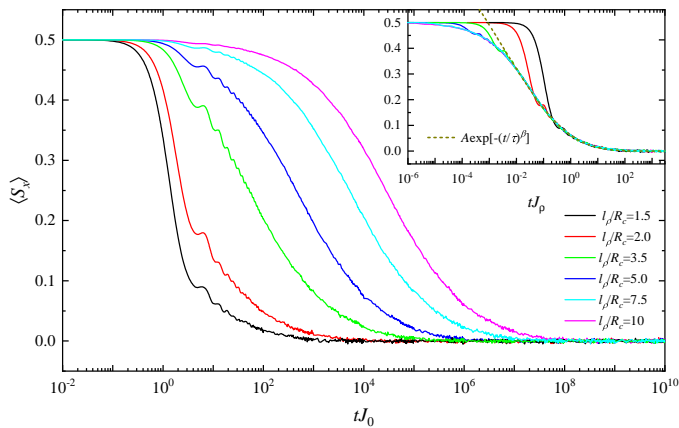


FIG. 5: Magnetization dynamics in a low-density Gaussian sample. Evolution curves of $\langle \hat{S}_x \rangle$ for six different values of l_ρ/R_c ranging from 1.5 to 10 are plotted. As l_ρ increases (ρ decreases), the initial fast decay seen in Fig. 4(a) shrinks along the time axis and a slow dynamics similar to that in Fig. 2 emerges. In the inset, the rescaled evolution curves ($tJ_0 \rightarrow tJ_\rho$) are shown, all of which fall onto a common one at the long-time part. We fit this common part to a stretched-exponential function (dashed dark yellow curve) and obtain an exponent of $\beta = 0.1817(9)$ and a decay rate of $\gamma = 343(15)J_\rho$.

nents β_h and decay rates γ_h for various values of l_ρ/R_c , which are plotted in Fig. 4(b). We observe a monotonic approach to the normal exponential decay ($\beta_h = 1$) from $\beta_h > 1$ with an increasing disorder in the system (see Fig. 3), while the decay rate γ_h increases from 0 to the order of J_0 .

2. Low-density regime

In the other regime with $l_\rho/R_c > 1$ ($\rho < 10^{12} \text{ cm}^{-3}$ for $R_c = 1 \mu\text{m}$), the pair interaction strengths distribute over a range covering 5 or 6 orders of magnitude (see Fig. 3). The results for dynamics of $\langle \hat{S}_x \rangle$ at six different values of l_ρ/R_c are shown in Fig. 5. As the cloud size w (l_ρ) increases, the initial collapse phase [see Fig. 4(a)] shrinks and a slow decay with an oscillating feature merges at long time, which is similar as that in Fig. 2(b).

We rescale the time t for each curve in Fig. 5 by the characteristic interaction strength J_ρ (as introduced in the beginning of this section), which is presented in the inset. The curves for different l_ρ/R_c fall onto a common one at the long-time part including the oscillation, which occupies a larger region in the dynamics for larger l_ρ/R_c and demonstrates a universal behavior. We fit this common long-time part of the $\langle \hat{S}_x \rangle$ dynamics to the stretched-exponential function $A \exp[-(\gamma t)^\beta]$ with the fitting parameter A, γ, β [dashed curves in the inset of Fig. 5]. The fitted exponent β is 0.1817(9) and the decay rate γ is $343(15)J_\rho \approx 19.5(9)J_0 F^{1/\beta_0}$ ($F \ll 1$). Both the stretched exponent and decay rate

are different from the values obtained analytically for a homogeneous sample with $\beta_0 = 0.5$ in Sec. II B, where $\beta = \beta_0 = 0.5, \gamma \approx 1.57J_0 F^{1/\beta_0}$.

III. CONCLUSION

In conclusion, we have considered magnetization relaxation of homogeneous and inhomogeneous samples of Ising spins with a soft-core pairwise potential. We have derived an analytic formula describing the whole dynamics in the homogeneous case, with three distinct relaxation regions in the time axis. The short-time dynamics follows $\exp(-kt^2)$ and stretched-exponential laws are found at long-time dynamics. As conjectured by Klafter and Shlesinger, this law arises from a scale-invariant distribution of relaxation times, which is only approximately fulfilled in the long-time limit since the soft-core potential in general is not scale-invariant. The breakdown of scale invariance is indicated by an oscillating feature in the relaxation between the short- and long-time limit.

Similar behaviours emerge for large Gaussian samples compared to the soft-core radius, where strong disorder presents in the system. However, for small Gaussian samples a coherent many-body dynamics is found since all spins interact with each other with an almost constant interaction strength. A smooth change from the coherent regime to the strongly disordered regime can be realized via tuning the Gaussian size of the sample. Our results in both homogeneous and inhomogeneous situations may stimulate experimental interests in the cold-atom community and may also be generalized to other types of interaction potentials.

Acknowledgements

We are grateful to Xiaopeng Li and the Rydberg team of Weidemüller's group in Heidelberg for careful reading of our manuscript. We are supported by the Anhui Initiative in Quantum Information Technologies. Y.H.J. also acknowledges support from the National Natural Science Foundation under Grant No. 11827806. M.W. is supported by the Deutsche Forschungsgemeinschaft (DFG, German Research Foundation) under Germany's Excellence Strategy EXC2181/1-390900948 (the Heidelberg STRUCTURES Excellence Cluster), within the Collaborative Research Center SFB1225 (ISOQUANT) and the DFG Priority Program 1929 "GiRyd" (DFG WE2661/12-1).

Appendix

$x = 1/y$ in the later integral, resulting in

Analytic derivation in a homogeneous sample

To derive Eq. (8a) from $I(J_0t; \beta_0) = \int_{y_0}^{J_0t} (J_0t/y - 1)^{\beta_0} \sin y dy$ for $\beta_0 < 1$, we first introduce a new variable

$$\begin{aligned}
 I(J_0t; \beta_0) &= \int_{1/(J_0t)}^{1/y_0} (J_0tx - 1)^{\beta_0} x^{-2} \sin(x^{-1}) dx \\
 &\xrightarrow{y_0 \rightarrow 0} \frac{(J_0t)^{\beta_0}}{2i} \int_{1/(J_0t)}^{\infty} \left(x - \frac{1}{J_0t}\right)^{\beta_0} x^{-2} (e^{ix^{-1}} - e^{-ix^{-1}}) dx \\
 &= \frac{(J_0t)^{\beta_0}}{2i} B(1 - \beta_0, 1 + \beta_0) (J_0t)^{1 - \beta_0} [{}_1F_1(1 - \beta_0, 2, iJ_0t) - {}_1F_1(1 - \beta_0, 2, -iJ_0t)] \\
 &= J_0t B(1 - \beta_0, 1 + \beta_0) \Im[{}_1F_1(1 - \beta_0, 2, iJ_0t)]
 \end{aligned} \tag{10}$$

Here we have used an integral formula listed in Ref. [21], which reads

$$\int_m^{\infty} x^{v-1} (x - m)^{\mu-1} e^{b/x} dx = B(1 - \mu - v, \mu) m_1^{\mu+v-1} F_1(1 - \mu - v, 1 - v, b/m), \tag{11}$$

and is valid for $m > 0, 0 < \Re(\mu) < \Re(1 - v)$. $\Re(z)$ represents the real part of z . The asymptotic behavior of the Kummer confluent hypergeomet-

ric function ${}_1F_1(a, b, z)$ at large $|z|$ is ${}_1F_1(a, b, z) \sim \Gamma(b)[e^z z^{a-b}/\Gamma(a) + (-z)^{-a}/\Gamma(b-a)]$, which gives rise to Eq. (8c).

-
- [1] K. Binder and A. P. Young, *Reviews of Modern Physics* **58**, 801 (1986).
 - [2] C. A. Müller and D. Delande, arXiv:1005.0915 [cond-mat, physics:quant-ph] (2016), comment: Notes of a lecture delivered at the Les Houches School of Physics on "Ultracold gases and quantum information" 2009 in Singapore. v3: corrected mistakes, improved script for numerics, Chapter 9 in "Les Houches 2009 - Session XCI: Ultracold Gases and Quantum Information" edited by C. Miniatura et al. (Oxford University Press, 2011), 1005.0915.
 - [3] N. Upadhyaya and A. Amir, *Physical Review Materials* **2**, 075201 (2018).
 - [4] E. J. Meier, F. A. An, A. Dauphin, M. Maffei, P. Massignan, T. L. Hughes, and B. Gadway, *Science* **362**, 929 (2018).
 - [5] S. Yu, C.-W. Qiu, Y. Chong, S. Torquato, and N. Park, *Nature Reviews Materials* **6**, 226 (2021), ISSN 2058-8437.
 - [6] J. C. Phillips, **59**, 1133 (1996), ISSN 0034-4885.
 - [7] J. Klafter and M. F. Shlesinger, *Proceedings of the National Academy of Sciences* **83**, 848 (1986), ISSN 0027-8424, 1091-6490.
 - [8] P. Schultzen, T. Franz, S. Geier, A. Salzinger, A. Tebben, C. Hainaut, G. Zürn, M. Weidemüller, and M. Gärttner, arXiv:2104.00349 [cond-mat, physics:quant-ph] (2021), 2104.00349.
 - [9] A. Signoles, T. Franz, R. Ferracini Alves, M. Gärttner, S. Whitlock, G. Zürn, and M. Weidemüller, *Physical Review X* **11**, 011011 (2021), ISSN 2160-3308.
 - [10] P. Schultzen, T. Franz, C. Hainaut, S. Geier, A. Salzinger, A. Tebben, G. Zürn, M. Gärttner, and M. Weidemüller, arXiv:2107.13314 [cond-mat, physics:quant-ph] (2021), 2107.13314.
 - [11] J. B. Balewski, A. T. Krupp, A. Gaj, S. Hofferberth, R. Löw, and T. Pfau, *New Journal of Physics* **16**, 063012 (2014), ISSN 1367-2630.
 - [12] A. Browaeys and T. Lahaye, *Nature Physics* **16**, 132 (2020), ISSN 1745-2481.
 - [13] A. L. Gaunt, T. F. Schmidutz, I. Gotlibovych, R. P. Smith, and Z. Hadzibabic, *Physical Review Letters* **110**, 200406 (2013).
 - [14] B. Mukherjee, Z. Yan, P. B. Patel, Z. Hadzibabic, T. Yef-

- sah, J. Struck, and M. W. Zwierlein, *Physical Review Letters* **118**, 123401 (2017).
- [15] W. Ketterle, D. S. Durfee, and D. M. Stamper-Kurn, arXiv:cond-mat/9904034 (1999), comment: Long review paper with ~90 pages, ~20 figures. 2 GIF figures in separate files (4/5/99 fixed figure), cond-mat/9904034.
- [16] G. G. Emch, *Journal of Mathematical Physics* **7**, 1198 (1966), ISSN 0022-2488, 1089-7658.
- [17] C. Radin, *Journal of Mathematical Physics* **11**, 2945 (1970), ISSN 0022-2488.
- [18] J. Schachenmayer, A. Pikovski, and A. M. Rey, *Physical Review X* **5**, 011022 (2015), ISSN 2160-3308.
- [19] J. G. Bohnet, B. C. Sawyer, J. W. Britton, M. L. Wall, A. M. Rey, M. Foss-Feig, and J. J. Bollinger, *Science* **352**, 1297 (2016), ISSN 0036-8075, 1095-9203.
- [20] J. Zeiher, J.-y. Choi, A. Rubio-Abadal, T. Pohl, R. van Bijnen, I. Bloch, and C. Gross, *Physical Review X* **7**, 041063 (2017).
- [21] I. S. Gradshteyn and D. Zwillinger, *Table of Integrals, Series, and Products* (Elsevier, Academic Press is an imprint of Elsevier, Amsterdam ; Boston, 2015), eighth edition ed., ISBN 978-0-12-384933-5.